THE DERIVATION OF ATMOSPHERIC OPACITY FROM SURFACE TEMPERATURE OBSERVATIONS.

R. J. Wilson , *NOAA/Geophysical Fluid Dynamics Laboratory, Princeton, NJ, USA (John.Wilson@noaa.gov)*,
J. Noble, *San Jose State University and NASA/Ames Research Center, Mountain View, CA, USA*,
S. J. Greybush, *University of Maryland, College Park, MD, USA.*

Introduction: The spatial and temporal variability of column integrated aerosol is a fundamental aspect of characterizing Martian weather and climate and is thus a critical observation from orbiting spacecraft. The dust and water ice cloud opacities retrieved from MGS TES nadir spectra (and archived in the Planetary Data System) have provided considerable insight into the dust and water cycles [*Smith*, 2004]. The TES column opacity retrievals require a clear thermal contrast between the surface and emitting air temperatures [*Smith et al*., 2001]. This condition is typically satisfied for observations over daytime surfaces free of CO_2 frost. In general, aerosols lead to a cooling of daytime (2pm) surface temperatures as the direct solar beam is attenuated, while nighttime (2am) surface temperatures are increased by the enhanced downward atmospheric radiation at the surface. For sufficiently dusty conditions, daytime surface and atmospheric temperatures can converge so that the required temperature contrast is lost. This condition was particularly common during the 2001 global dust storm. Here we describe a technique that provides a more robust estimation of column aerosol opacity, one that appears to work well for both daytime and nighttime conditions.

This work was motivated by the desire to create gridded column opacity maps of the expansion period of the 2001 global dust storm [*Cantor*, 2007; *Wilson et al*. 2008]. We are finding that identifying the influence of aerosol on surface temperature is also useful for deriving column opacities from MRO Mars Climate Sounder (MCS) observations. MCS is an infrared radiometer using limb and on-planet viewing. The limb profiles allow temperature and aerosol retrievals from 5-10 km to ~80 km in height [*Kleinbohl et al*. 2009]. A notable limitation of MCS is the current inability to retrieve column aerosol opacity. Moreover, during periods of moderate to high opacity it is not be possible to retrieve aerosols and temperatures near the surface. Hence an independent capability of deriving column optical thicknesses is desirable.

Global maps of surface thermal inertia have previously been derived by fitting observed surface temperatures to a thermal model of the surface [*Putzig et al*., 2005]. This process requires knowledge of atmospheric opacity, so the fitting is carried out for relatively clear-sky conditions. Here, we use a Mars general circulation model (MGCM) which self consistently predicts surface and atmospheric temperatures for different dust and water ice cloud distributions. We create an ensemble of runs and derive the dust and/or ice opacities that yield the best fits with the observations. We anticipate that this technique can be readily incorporated and automated in ensemble-based data assimilation systems [*Hoffman et al*., 2010].

Methodology: In practice, observed surface temperatures are actually top-of-atmosphere brightness temperatures in spectral regions that are relatively transparent to the atmosphere. The archived TES surface temperatures are represented by brightness temperature at 1300 cm^{-1} (7.7 μm) for temperatures greater than 220 K and by the minimum brightness temperature between 20-33μm for temperatures less than 210 K (assuming a uniform surface emissivity of 0.97). A blending of the two measures is used for temperatures between 210 and 220 K. MCS provides on-ground observations in the 32 μm channel, which is somewhat more transparent to dust than the 23 μm region but is less transparent than the 7 μm region. MCS on-planet views typically have a slant path with a ~2.5 airmass factor. The GFDL MGCM is used to calculate top-of-the atmosphere brightness temperatures to compare with spacecraft observations. The model uses a radiation code based on a two-stream solution to the radiative transfer equation. Fluxes and heating rates are calculated using appropriate aerosol optical properties at solar and infrared wavelengths [*Wilson*, 2011]. Top-of-atmosphere radiances are calculated at 7, 23 and 32 μm (T_7, T_{23}, and T_{32}) to compare with the observed brightness temperatures for TES and MCS. The T_{32} temperature is calculated along a slant path equivalent to the viewing angle of MCS off-limb (on-ground) viewing. We have derived a surface thermal inertia field at 2°x2° resolution to allow the MGCM to predict the observed morning and afternoon brightness temperatures in seasons and locations where our assumptions of atmospheric opacity are well founded [*Wilson and Smith*, 2006; *Wilson et al*. 2007]. We run an ensemble of MGCM simulations with a range of aerosol opacities selected to "bracket" the possible state of the atmosphere as it evolves in time.

Results: The opacity derivation is illustrated in Figure 1, which shows observed and simulated brightness temperatures along a daytime orbit that passes over an area (southward of ~25°S) where MOC imagery indicates the presence of thick dust cloud. TES temperatures are shown in the top panel, along with those from an ensemble of MGCM simu-

lations employing different values of fixed dust opacity (τ= 0.2, 0.5, 1.0, 2.0, 3.0, 4.0, and 5.0). The simulated daytime brightness temperatures show the expected decrease with increasing optical depth. A best-fit opacity is obtained by interpolation among the ensemble temperatures. The bottom panel of figure 1 compares the retrieved opacities from the PDS archive and the opacities derived from the brightness temperature. The two opacity estimates agree nicely for latitudes with a good temperature contrast between the surface and atmosphere. The TES retrieval clearly fails in the very dusty region south of the dust cloud edge at 25°S, while the derived opacity estimates appear to be quite reasonable. Note that south of the polar cap edge at ~60°S, the observed brightness temperatures exceed the temperature (146-148°K) expected for CO_2 ice. This signature of dust over the south polar cap is in agreement with MOC images.

Figure 2 shows the time evolution of observed 2am and 2pm brightness temperatures at a location on the equator during the development of the 2001 global dust storm. The 2pm opacity observations from the PDS archive are shown in the bottom panel. The rapid onset of the storm is evident in the abrupt increase in nighttime temperatures and decrease in daytime temperatures. Figure 2c shows the resulting fittings for both 2am and 2pm opacity. The fitted 2pm opacities are in very close agreement with those retrieved by the TES team, while the 2am opacities also appear to be quite plausible estimates that would otherwise be unavailable. Our interpretation is that this region experienced a rapid increase in opacity between L_s=185 and 188° associated with the eastward expansion of an elevated tropical dust plume. It is reasonable that there would be relatively little diurnal opacity variation with such a feature.

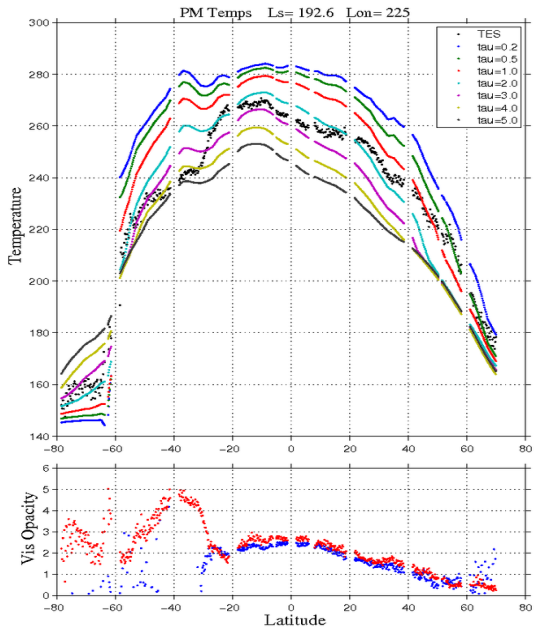

Figure 1. (a) Observed and simulated daytime brightness temperatures for Storm Day 29 along an orbit track roughly at 225° E. TES. Observed temperatures are shown as black dots while MGCM simulation results are color-coded by visible opacity. (b) PDS archived (blue) and derived (red) column opacity estimates.

Figures 1 and 2 show that the MGCM ensemble provides a measure of the sensitivity of the simulated brightness temperatures to changes in opacity, which can be used to provide error bounds on the derived opacity. We expect that this feature will prove to be especially valuable for the incorporation of this method in ensemble-based data assimilation systems.

We have been overlaying the newly fitted opacities on MOC imagery to aid in the creation of gridded opacity fields for describing the development of the 2001 global dust storm. Figure 3 shows that the fitting technique is able to provide significantly greater coverage of the dust storm. The imagery provides a guide for the interpolation of opacity between adjacent orbits. Our experience is that derived and retrieved (PDS) opacities are generally in very good agreement for conditions when retrieved opacities are available. However, we did find a particularly interesting exception when fitted and retrieved opacities in the Daedalia region diverged shortly after the start of significant dust lifting in that region. It appears that a real decrease in surface

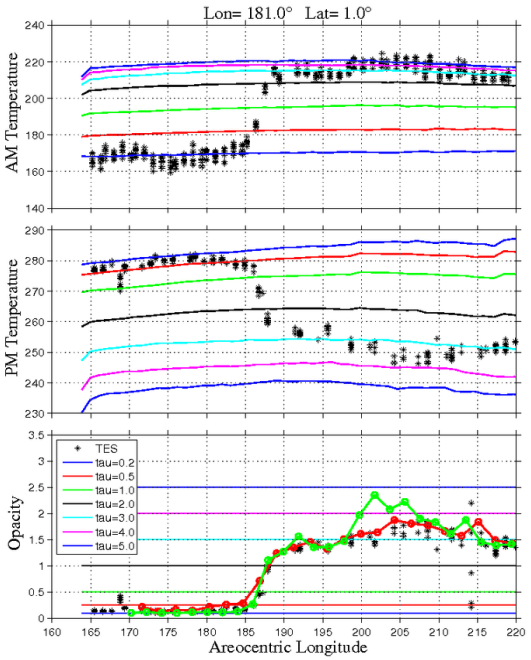

Figure 2. (a) The evolution of observed (black stars) and simulated 2am brightness temperatures for a location in Lucas Planum during the 2001 global dust storm. Seven simulation runs are shown with solid colored lines. (b) The corresponding 2pm brightness temperatures. (c) The corresponding pressure normalized 2pm column optical depths. The red curve shows the derived IR optical depth obtained by interpolating among the 2pm MGCM simulations and the green curves shows the corresponding 2am opacity estimates. Note that the figure legend indicates the visible optical depths for reference simulations.

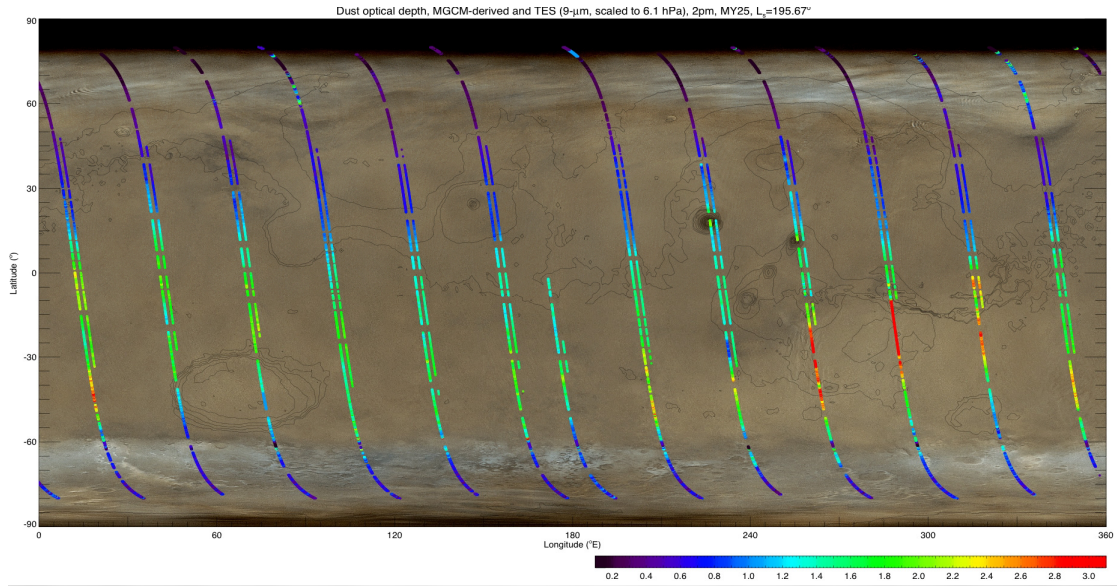

Figure 3. MOC image of global dust storm at L_s = 195.7° (storm day 35) with overlayed spacecraft orbit tracks color-coded by IR dust column opacity. Both TES-retrieved and MGCM-derived opacity estimates (right and left elements of orbit track pairs) are shown. Note that TES retrieved opacities are missing in regions where dust opacity is relatively high. The anomalous low opacity region at 240° E, 29°S in the derived data set (relative to TES) is attributed to a rapid decrease in surface albedo at this location.

albedo in this region leads to increased daytime temperature, which the fitting process compensates for by underestimating the dust necessary to depress simulated temperatures to the values observed. We attribute the sudden decrease in albedo in this region to dust removal from the surface soon after the onset of dust lifting.

We have begun using MCS 32 μm brightness temperatures to estimate aerosol opacity during the MRO mission. Relative to TES daytime nadir observations, the longer slant path, less transparent wavelength (32 vs. 7 μm), and cooler time of day (1500 vs 1400 LT) make MCS a somewhat less sensitive opacity detector. For example, we are finding that MCS afternoon temperatures appear to be more sensitive to water ice clouds than was the case for TES. However, the fitting technique appears to provide useful results. Figure 4b compares the evolution of daytime brightness temperatures in Thaumasia during MY29 with an ensemble of MGCM simulations. The visible opacities evidently spike up from ~0.8 to well above 2 before relaxing back to ~1. The progression of this regional storm, from the initial outbreak in Chryse to further lifting south and west in Thaumasia and subsequently in Cimmeria and Promethei, can be followed in both the morning and afternoon temperature anomaly fields and is consistent with that seen in MARCI images [*Malin et al.*, 2009]. We are currently using the derived column opacity estimates, the limb aerosol retrievals and

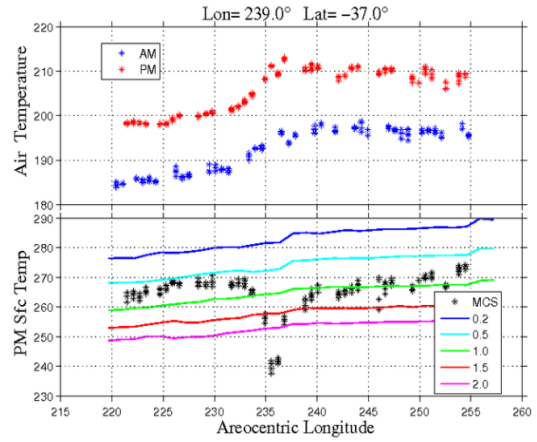

Figure 4. (a) Evolution of air temperature (~0.3 mb) in the Thaumasia region at the time of the 2009 regional dust storm in MY29. (b) Observed and simulated daytime 32 μm brightness temperatures.

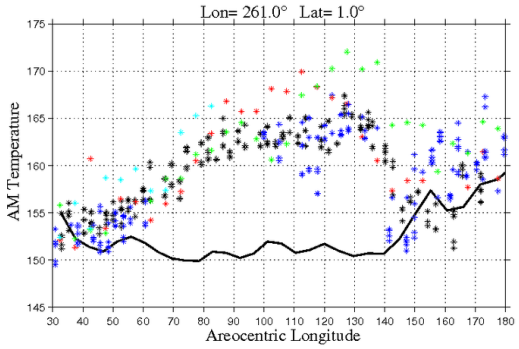

Figure 5. The seasonal evolution of morning temperatures at a location (4x4 degrees) in the Tharsis region. MCS 32 μm (0300 LT) temperatures are shown in blue and black for MY29 and MY30, respectively. TES 20 μm (0200 LT) temperatures are shown in cyan, red, and green. The black curve shows a reference 32 μm temperature from a MGCM simulation employing the observed TES dust column opacity and radiatively passive water ice clouds. The warming is attributed to the radiative influence of water ice clouds.

MARCI images to map out the development of this storm.

Water ice clouds also influence surface temperature. Figure 5 shows the evolution of morning (0300 LT) temperature at a location east of Pavonis Mons. The corresponding simulated brightness temperature is also shown, based on relatively clear-sky conditions and no radiatively active water ice clouds. It was argued in *Wilson et al*. [2007] that the rise and fall of the difference between the observed and simulated reference temperature is evidence for an evolving downward IR flux contribution from water ice clouds. Figure 6 shows the difference in observed and simulated brightness temperature around NH summer solstice. The same temperature anomaly pattern is seen in TES (~ 20 µm, 0200 LT) temperature data in this season and has been attributed to the enhanced IR radiation from nighttime clouds [*Wilson et al*., 2007]. We are currently working to fit the observed brightness temperatures by comparing with simulated temperatures from an ensemble of MGCM runs with varying cloud descriptions. Cloud opacities of ~1 appear to yield sufficient additional IR flux at the surface to account for the observed brightness temperature increase at solstice.

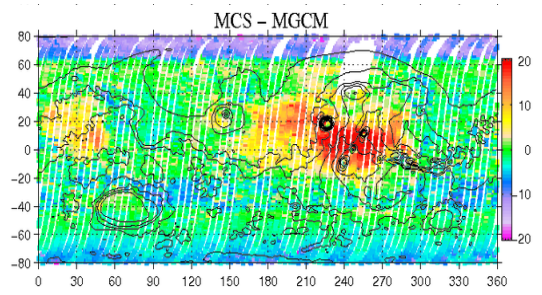

Figure 6. The difference between observed and simulated nighttime (3am) 32 µm temperatures. The season is L_s=105-110° in MY29.

Summary and Future Work: The fitting of simulated surface brightness temperatures to observed brightness temperatures appears to be a more flexible technique for estimating opacity than the TES opacity retrievals. We have found that the technique works well for daytime opacity estimation during the 2001 global dust storm and in other seasons viewed by TES. This technique allows estimation of opacity for both daytime and nighttime conditions, as well as over the polar caps. Preliminary results indicate that the technique works with MCS brightness temperatures as well. The results are best for cases with moderate to high aerosol opacity, which are the conditions for which standard MCS retrievals are least effective for assessing aerosol column opacity.

Work has begun on implementing this idea in a data assimilation system [*Greybush et al*., 2011]. The ensemble Kalman filter provides an ideal framework for generating time evolving gridded maps of dust opacity as part of a reanalysis. Using the covariance between ensemble perturbations of modeled dust opacity and brightness temperature, as well as the increment between observed and modeled brightness temperature, the system analyzes opacity values at each grid point as the optimal linear combination of opacity values from the ensemble.

Acknowledgments: This work was supported by a grant from the NASA Mars Data Analysis program. We thank Bruce Cantor at Malin Space Science Systems for access and interpretation of MOC imagery.

References:

Cantor, B.A. (2007), MOC observations of the 2001 Mars planet-encircling dust storm, *Icarus*, 186, 60-96, doi:10.1016/j.icarus.2006.08.019.

Greybush, S.J., et al. (2011), Martian atmosphere data assimilation of TES and MCS retrievals, 4th International Workshop on the Mars Atmosphere: Modeling and Observations, Paris.

Hoffman, M.J, S.J. Greybush, R.J. Wilson, et al. (2010), An ensemble Kalman filter data assimilation system for the martian aJtmosphere: Implementation and simulation experiments, *Icarus*, doi:10.1016/j.icarus.2010.03.034.

Kleinböhl, A., et al. (2009), Mars Climate Sounder limb profile retrieval of atmospheric temperature, pressure, and dust and water ice opacity, *J. Geophys. Res., 114*, E10006, doi:10.1029/2009JE003358.

Malin, M.C., et al., (2009) MRO MARCI Weather Report for the week of 30 March 2009-5 April 2009, Malin Space Science Systems captioned image release, MSSS-7.

Putzig, N.E., M.T. Mellon, K.A. Kretke, and R.E. Arvidson (2005), Global thermal inertia and surface properties of Mars from the MGS mapping mission, *Icarus*, *173*, 325-34

Smith, M.D. (2004), Interannual variability in TES atmospheric observations of Mars during 1999-2003, *Icarus*, *108*, 148-165.

Smith, M.D., et al. (2001), One martian year of atmospheric observations by the Thermal Emission Spectrometer, *Geophys. Res. Lett., 28*, 4263-4266.

Wilson, R.J. and M.D. Smith (2006), The effects of atmospheric dust on the seasonal variation of martian surface temperature, Second Mars modeling workshop, Granada, Spain.

Wilson, R.J., G. Neumann, and M.D. Smith (2007), The diurnal variation and radiative influence of martian water ice clouds, *Geophys. Res. Lett*., *34*, L02710, doi:10.1029/2006GL027976.

Wilson, R.J., et al. (2008), Simulation of the 2001 planet-encircling dust storm with the NASA/NOAA Mars general circulation model, Abstract 9023, Mars Atmosphere: Modeling and Observations Workshop, Williamsburg, VA.

Wilson, R.J. (2011), Dust cycle modeling with the GFDL Mars general circulation model, 4th International Workshop on the Mars Atmosphere: Modeling and Observations, Paris.